Electronic Supplementary Material (ESI) for Journal of Materials Chemistry A.

An Unprecedented Polyoxometalate-Encapsulated Organo-Metallophosphate Framework as Highly Efficient Cocatalyst for CO_2 Photoreduction

Ze-Yu Du,[a] Ying-Nan Xue,[a] Xiao-Mei Liu,[a] Ning-Fang Li,[a] Ji-Lei Wang,[a] Hua Mei[a] and Yan Xu*[a]*

Corresponding authors: Yan Xu and Hua Mei

E-mails: yanxu@njtech.edu.cn and meihua@njtech.edu.cn

Contents

Section 1. Crystal Structure

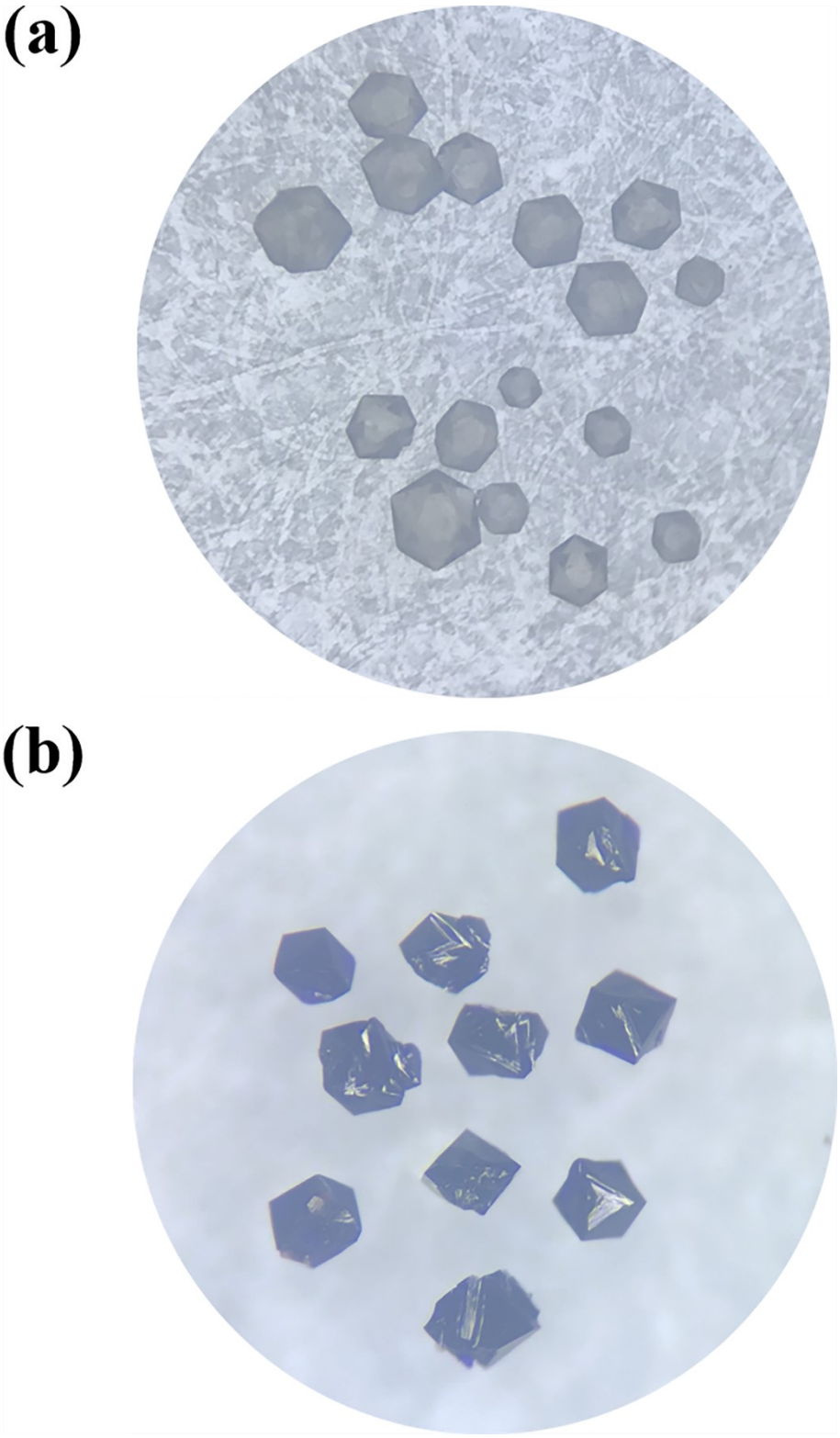

Fig. S1. (a) The crystal image of compound **1** under optical microscope; (b) the crystal image of compound **2** under optical microscope.

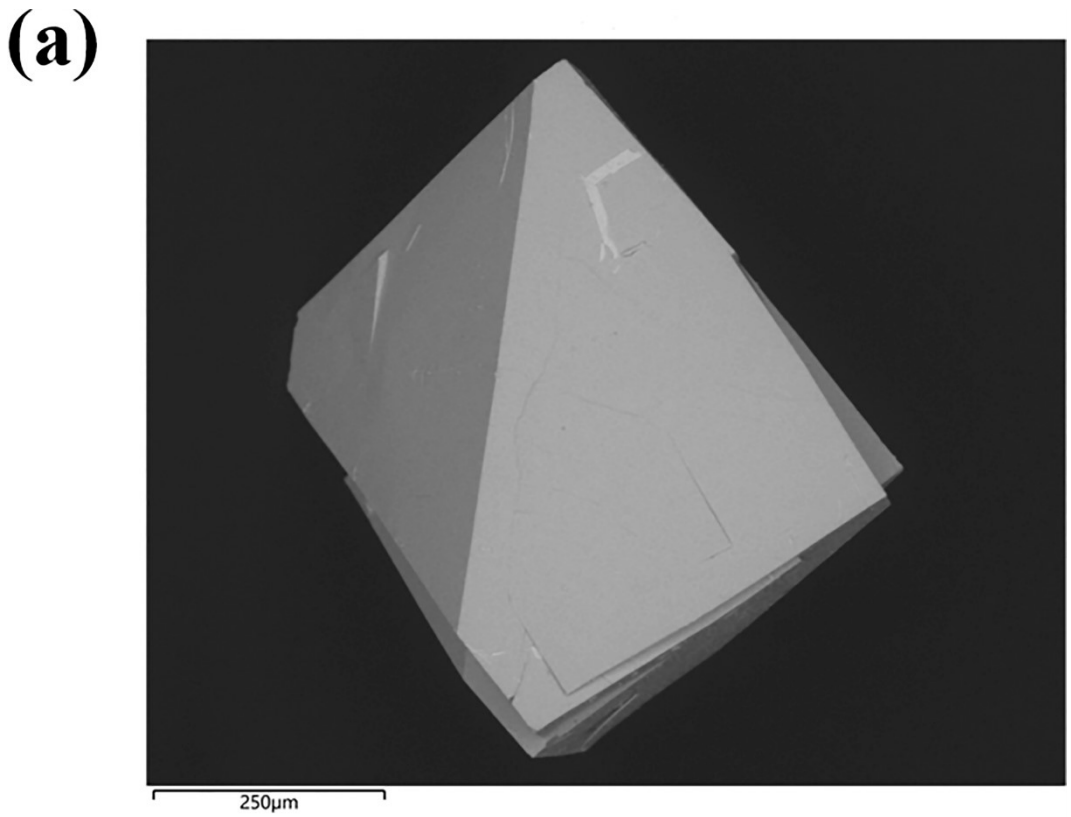

Fig. S2. (a) SEM image of compound **1**; (b) SEM image of compound **2**.

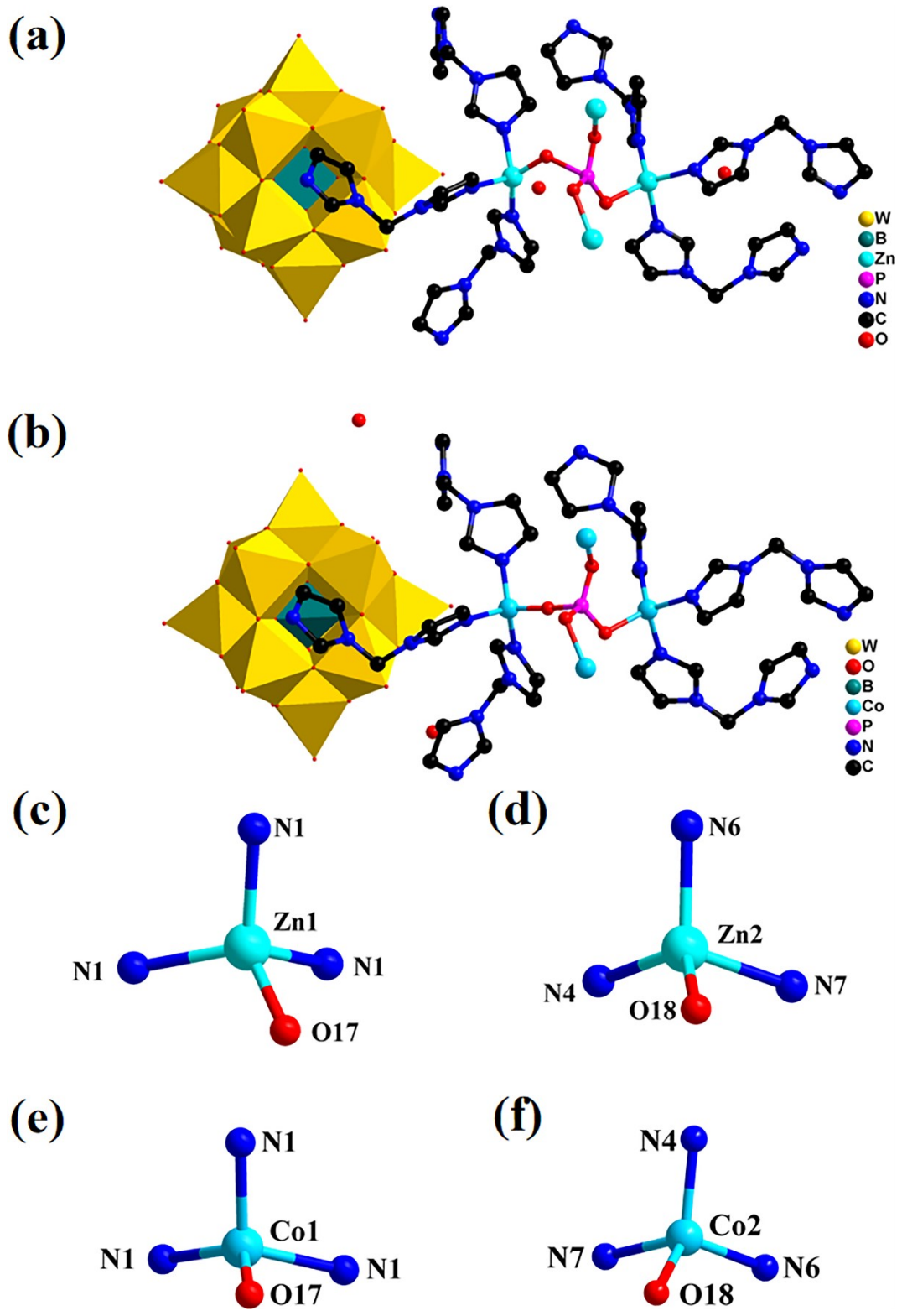

Fig. S3. (a) Stick and polyhedral representation of basic unit for compound **1**； (b) stick and polyhedral representation of basic unit for compound **2**; (c)/(d) the coordination environment of Zn atom in compound **1**; (e)/(f) the coordination environment of Co atom in compound **2**. The Hydrogen atoms are omitted for clarity.

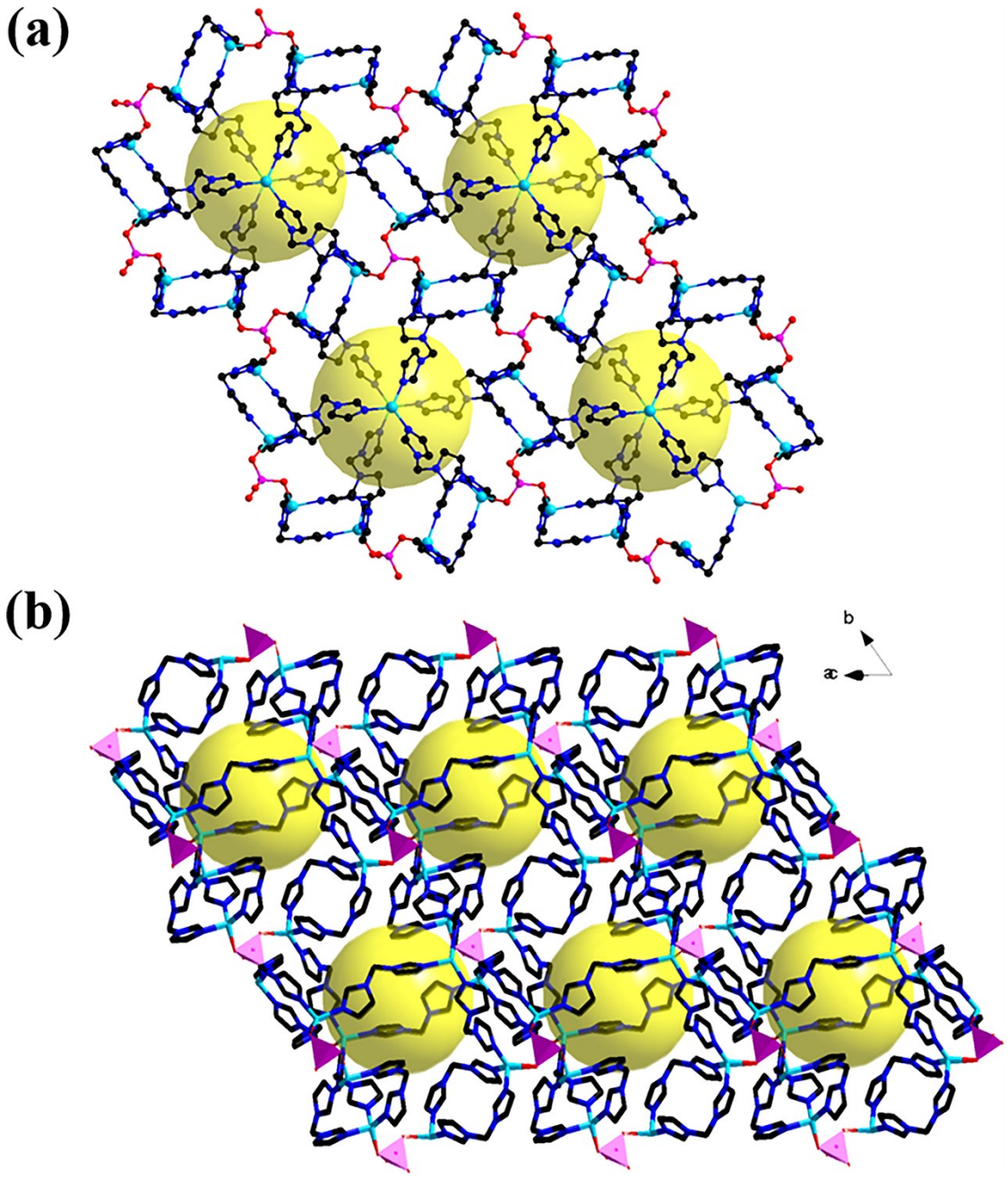

Fig. S4. (a) The 2D structure of the organo-metallophosphate frameworks；(b) the 3D structure of the organo-metallophosphate frameworks. Hydrogen atoms are omitted for clarity.

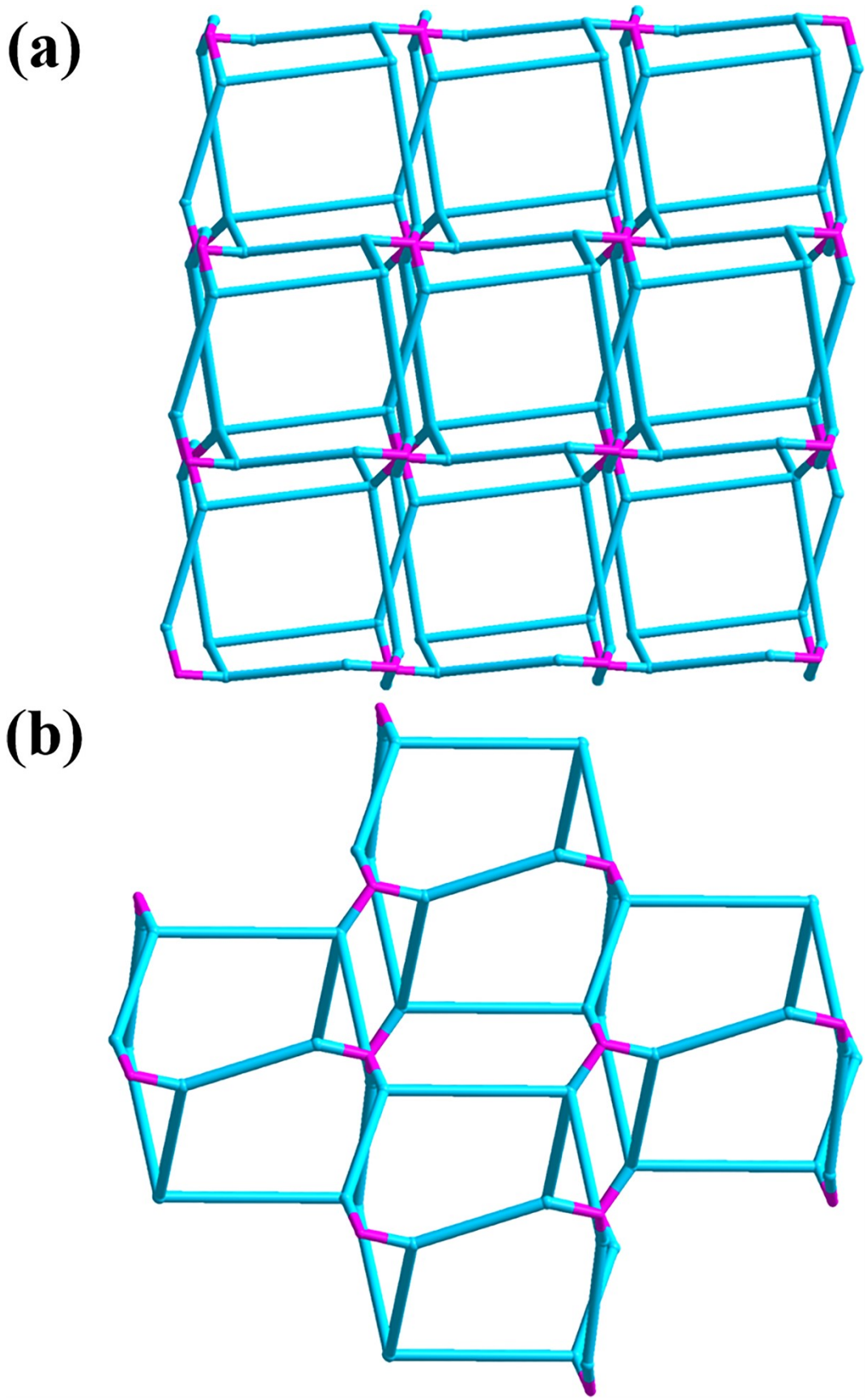

Fig. S5. (a)/(b) Topological features of organo-metallophosphate frameworks along the different direction.

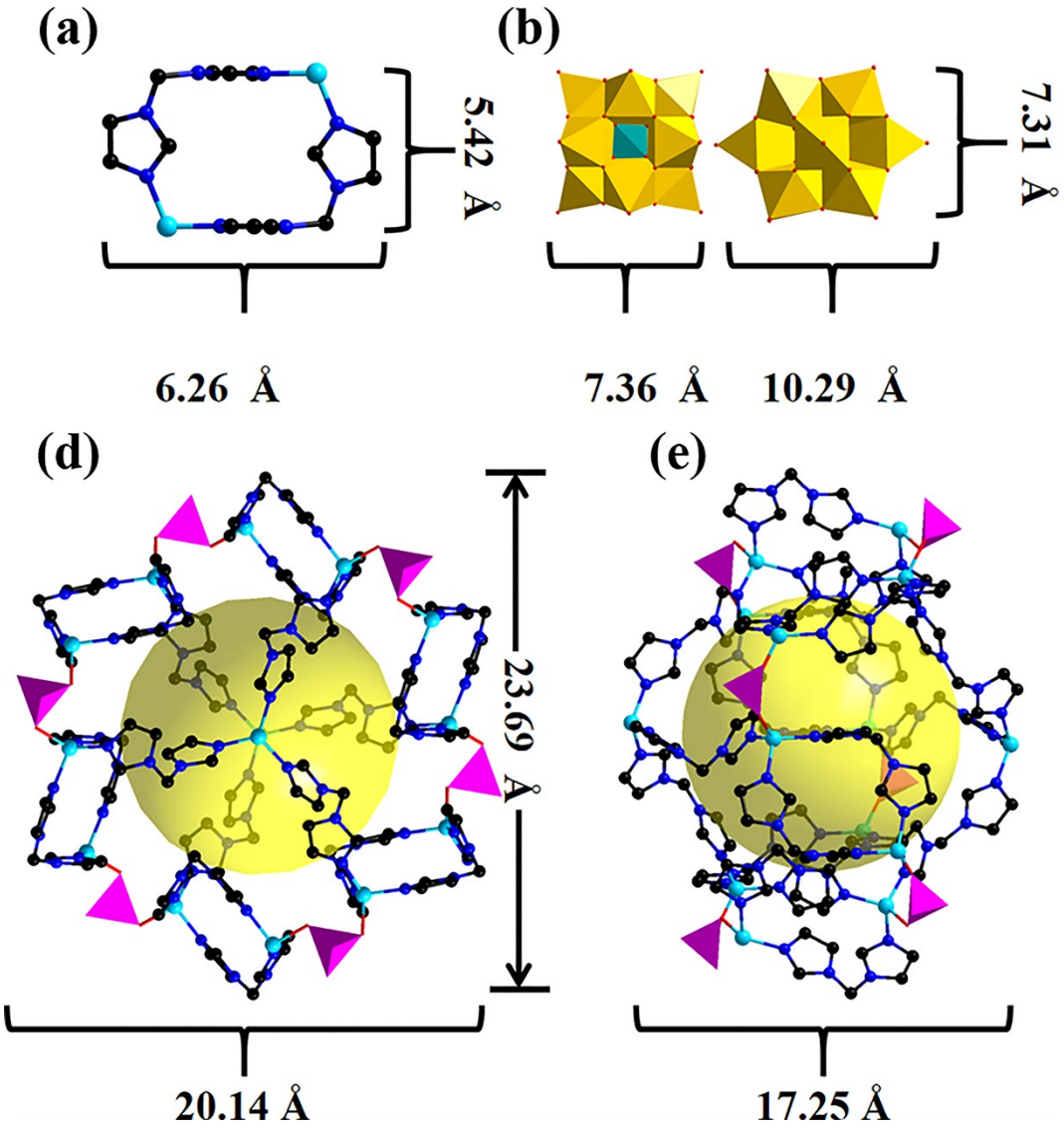

Fig. S6. Size perspective of the assembled structure for compound **2**.

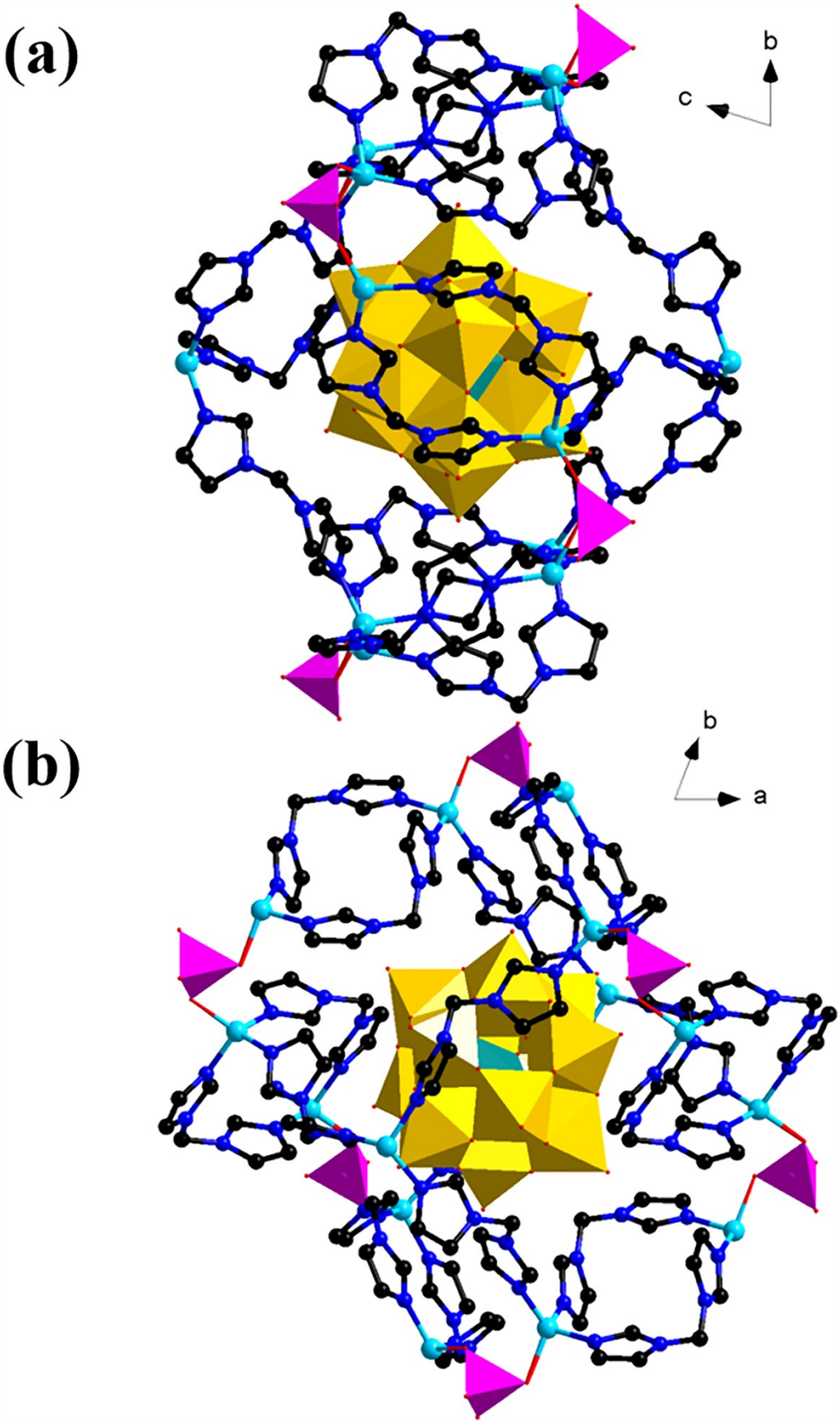

Fig. S7. Stick and polyhedral representation of 0D structure for compound **2** along the different direction.

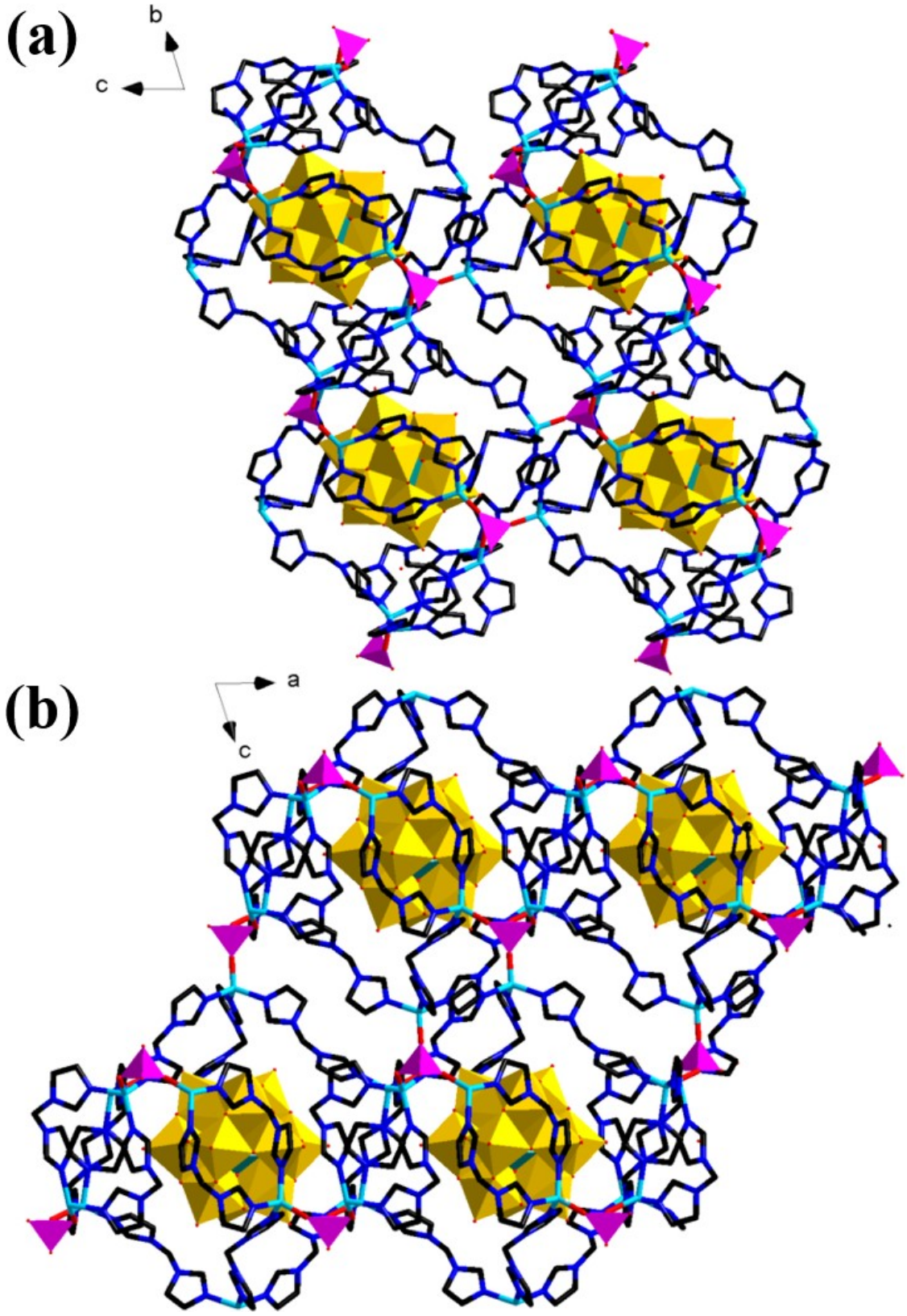

Fig. S8. (a) Stick and polyhedral representation of 3D structure for compound **2** along *a* axis. (b) stick and polyhedral representation of 3D structure for compound **2** along *b* axis.

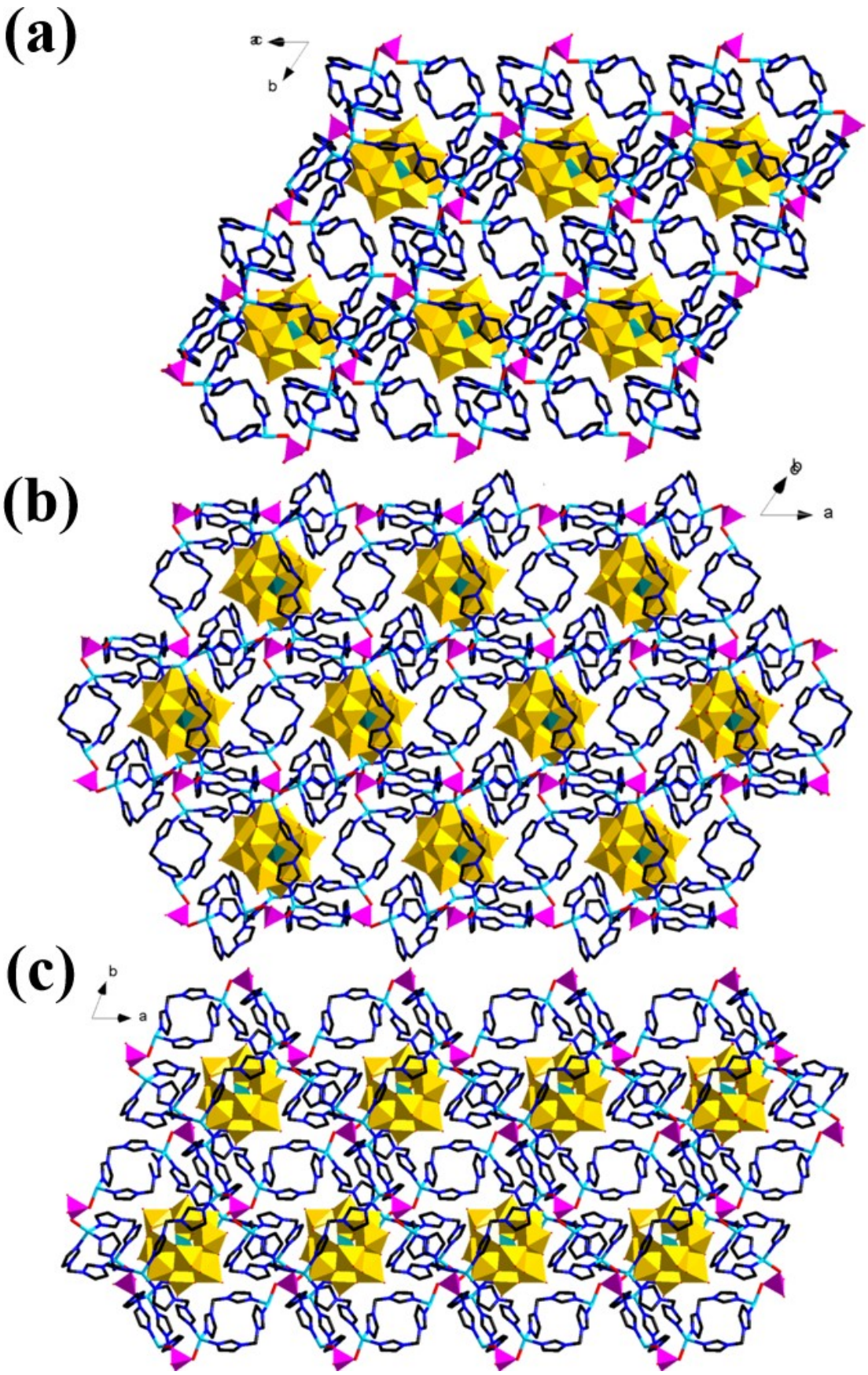

Fig. S9. (a)/(b)/(c) Stick and polyhedral representation of 3D structure for compound **2** along the different direction.

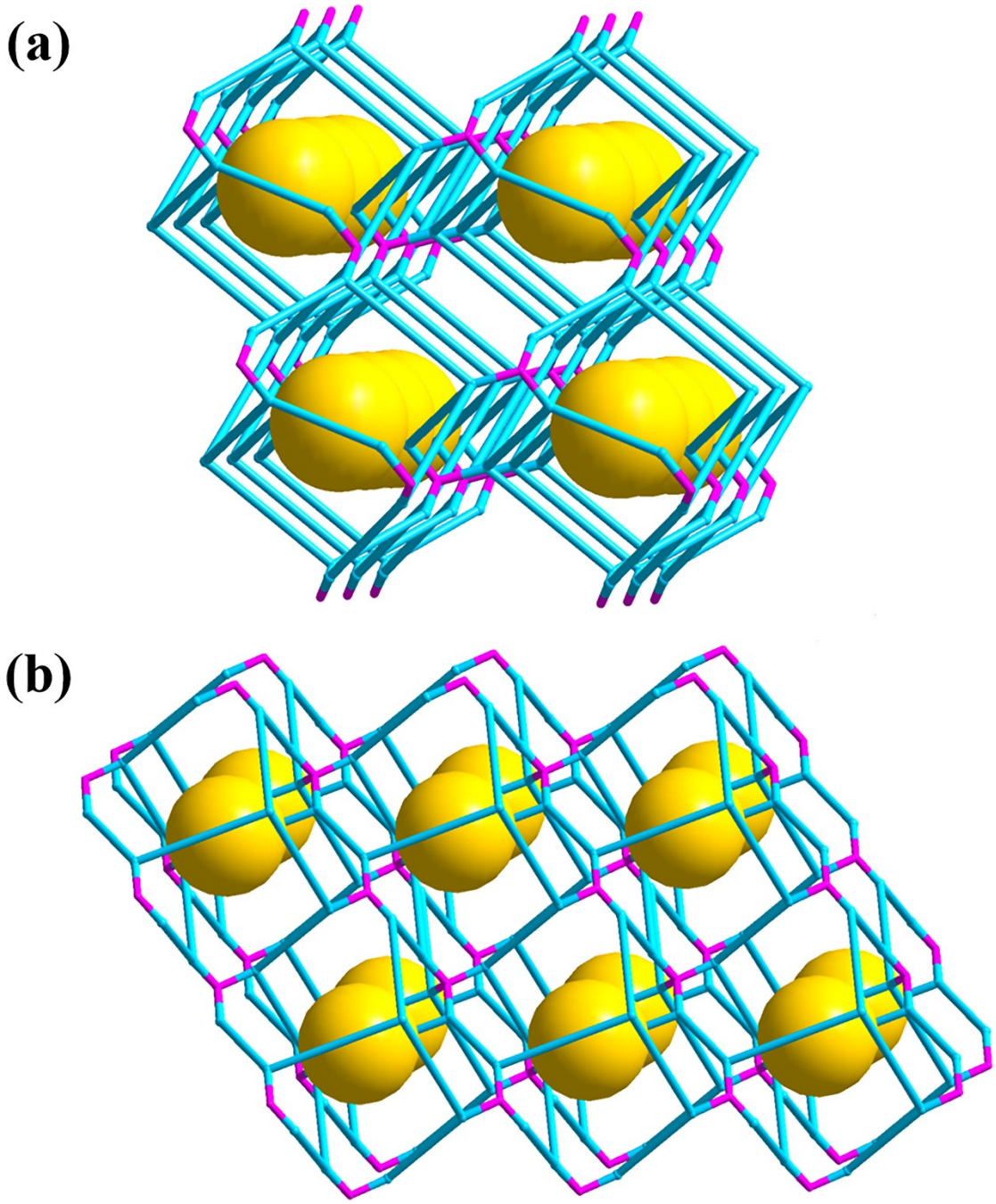

Fig. S10. Simplified structure of compound **2** viewing along the different direction. Gold balls represent POMs.

Section 2. Characterizations

Materials

$CoCl_2 \cdot 6H_2O$ (AR, ≥ 99.0%), $ZnCl_2$ (AR, ≥ 98.0%), and Na_2HPO_4 (AR, ≥ 99.0%) were bought from Sinopharm Chemical ReagentCo., Ltd. [Ru(2,2'-bipyridine)$_3$]$Cl_2 \cdot 6H_2O$ (98.0 %) was bought from Aladdin. Triethanolamine (AR, ≥ 78.0 %) and acetonitrile (AR, ≥ 99.8%) were purchased from Shanghai Ling Feng chemical agent Ltd. Nafion solution (5 wt %) was purchased from Sigma-Aldrich. Carbon dioxide (CO_2, 99.999%) gas was supplied by Jiangsu Tianhong Chemical Co., Ltd, the $13CO_2$ (99%) was purchased from Guangzhou Puyuan Gas Co., Ltd.

Characterization

X-ray diffraction (PXRD) data of two compounds was carried out on Smartlab TM 9KW diffractometer using Cu Kα radiation (λ = 1.54056 nm), and the range was 5 to 50 °. FTIR spectrums were performed on Nicolet 470 FTIR spectrometer with KBr pellets in the 400 - 4000 cm^{-1} range. Thermogravimetric analysis (TGA) was completed on STA449F3 thermogravimetric analyzer in N_2 atmosphere with a heating rate of 10 °C/min. The UV-vis diffuse reflectance spectra were investigated via SHIMADZU UV-2600 spectrophotometer, and the wavelength was in range of 200–800 nm. The SEM were identified by using a Hitachi TM 3000 scanning electron microscope at an accelerating voltage of 20 kV. Elemental analyses (C, N and H) were determined by a Perkin-Elmer 2400 elemental analyzer.

XRD

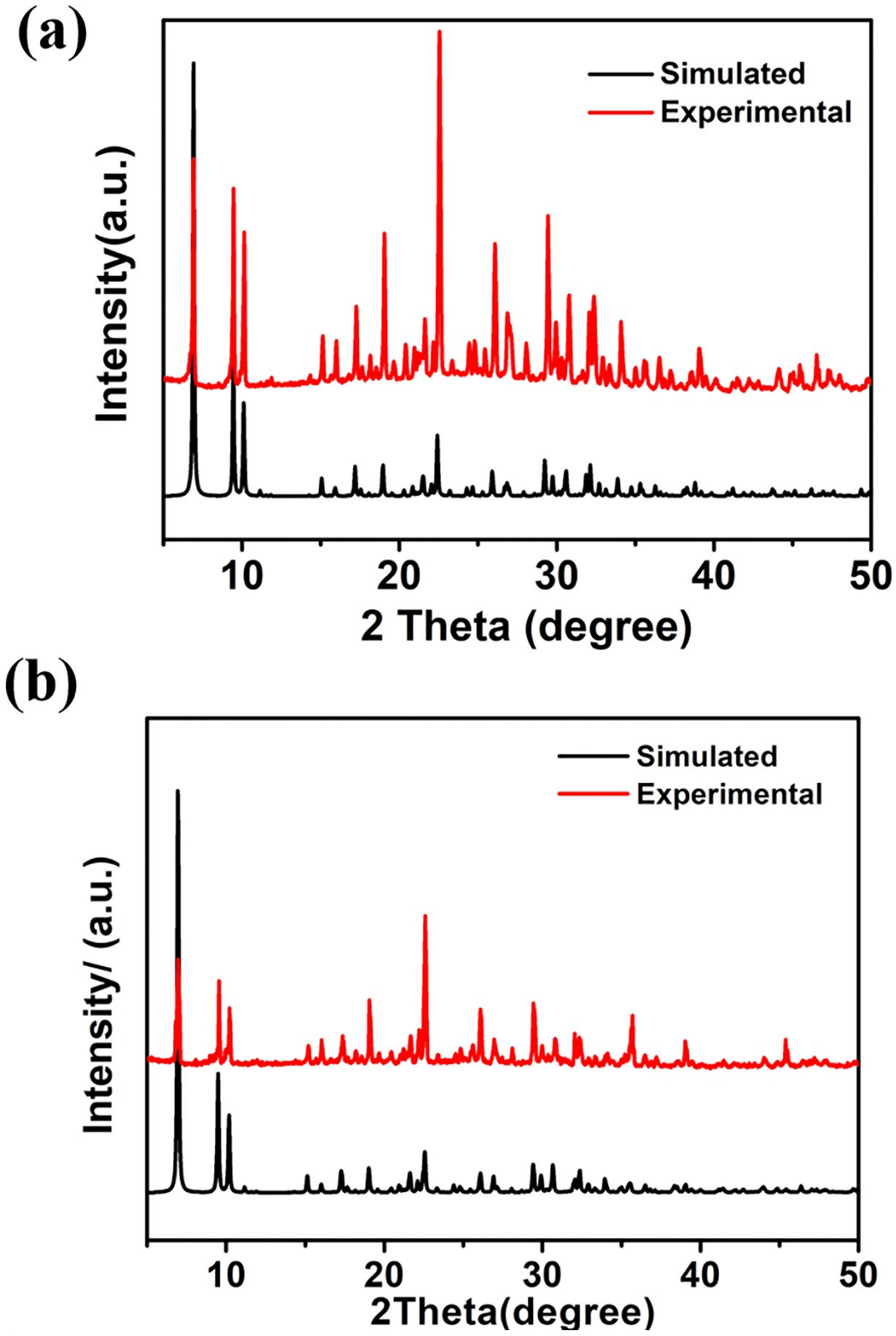

Fig. S11. The XRD pattern of (a) compound **1** and (b) compound **2**.

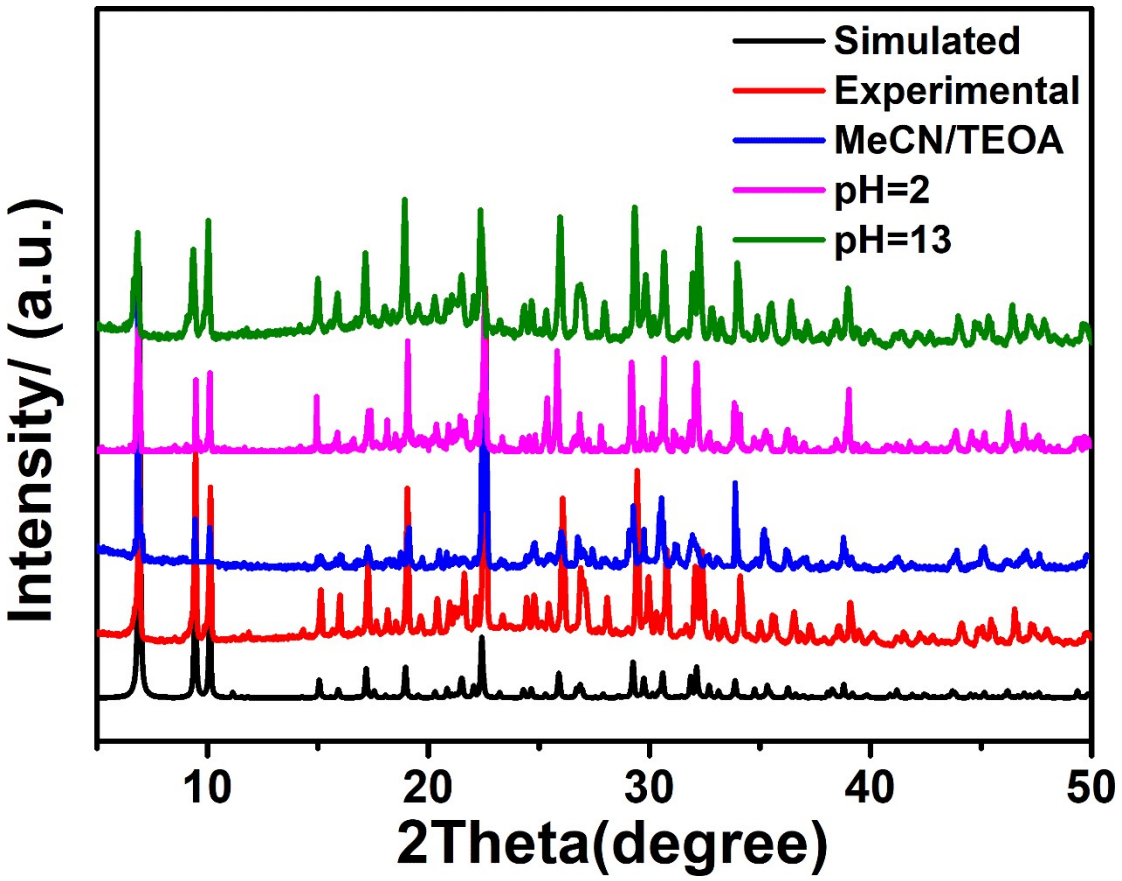

Fig. S12. XRD patterns of compound **1** in different solutions compared with simulated curves.

IR

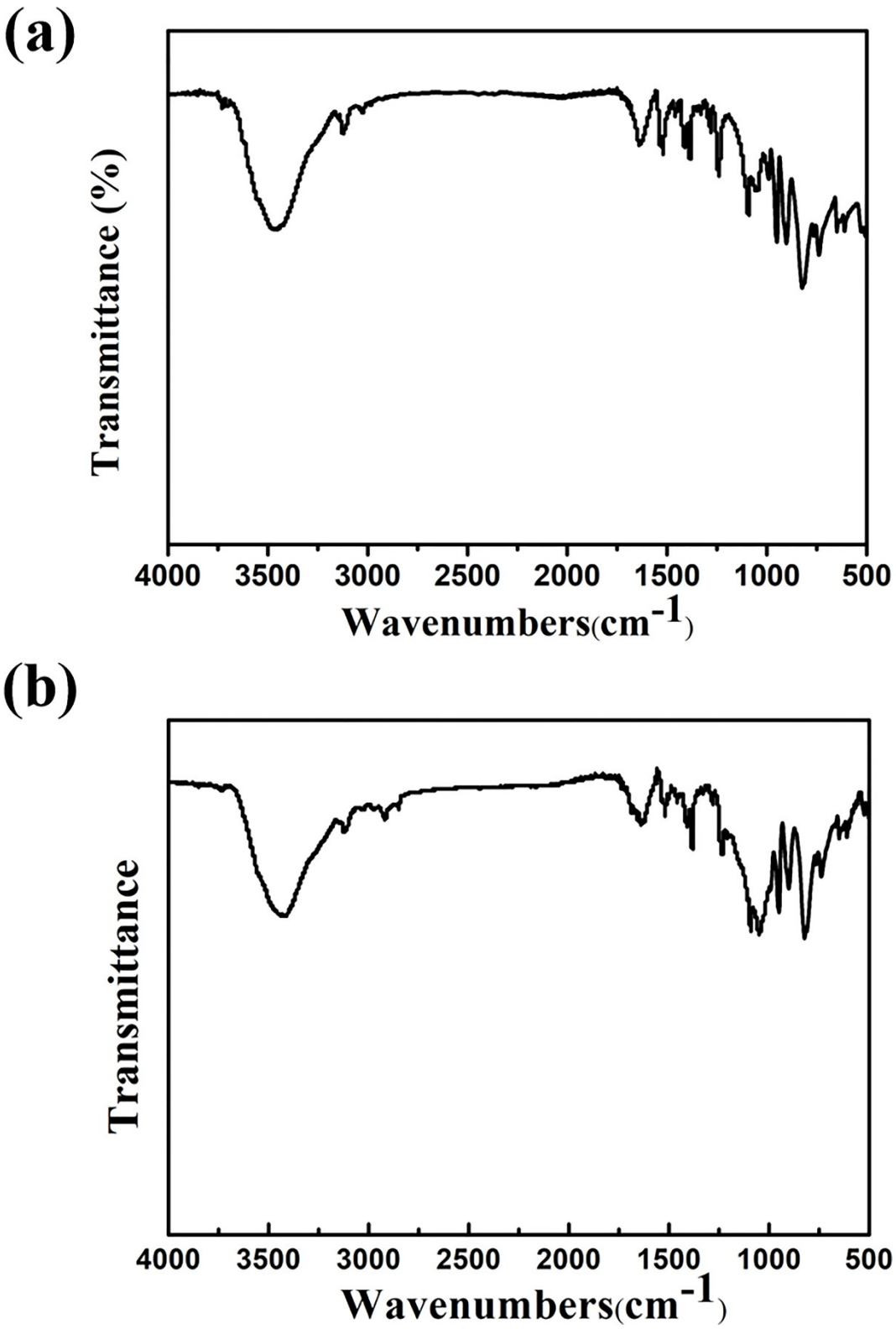

Fig. S13. The IR pattern of (a) compound **1** and (b) compound **2**.

TG

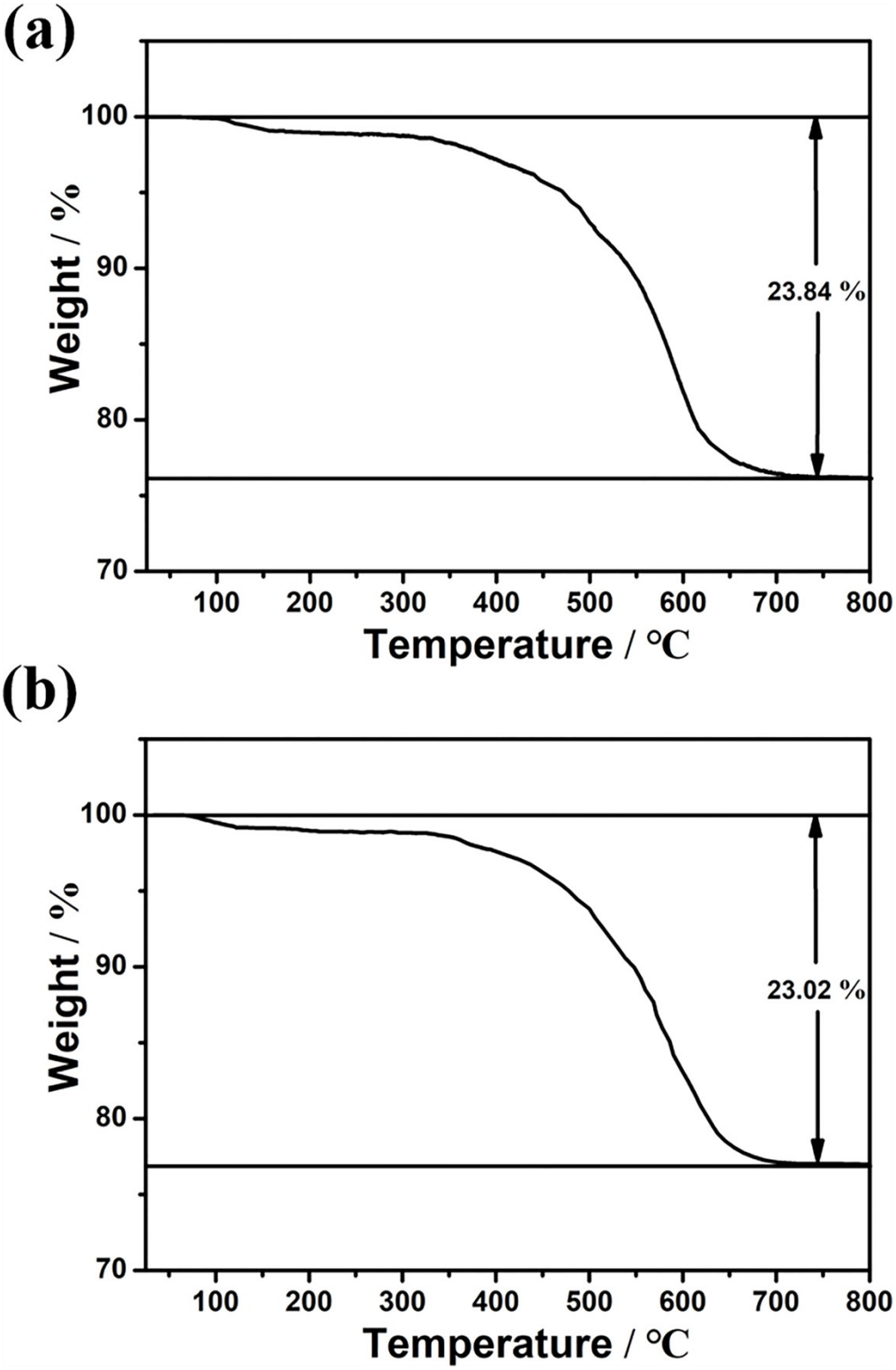

Fig. S14. The TG pattern of (a) compound **1** and (b) compound **2**.

Section 3. The Procedure of the CO_2 Photoreduction

Electrochemical measurements.

The Mott–Schottky spots were carried out at ambient environment via using the electrochemical workstation (CHI 760e) in a standard three-electrode system: The carbon cloth (CC, 1 cm×1 cm) modified with catalyst samples, carbon rod and Ag/AgCl were used as the working electrode, counter electrode and the reference electrode, respectively. The catalyst of 5 mg was grinded to powder and then dispersed in 1 mL of 0.5% Nafion solvent by ultrasonication to form a homogeneous ink. Subsequently, 200 μL of the ink were deposited onto the carbon cloth, and dried in room temperature for Mott-Schottky spots measurements. The Mott-Schottky plots were measured over an alternating current (AC) frequency of 1000 Hz, 1500 Hz and 2000 Hz, and three electrodes were immersed in the 0.2 M Na_2SO_4 aqueous solution.

Photocurrent responsive measurements.

The photoelectrochemical characterizations were performed on the electrochemical workstation (CHI 760e) with the assembled photoelectrodes as the working electrode, the Pt mesh as the counter electrode and the Ag/AgCl as the reference electrode. Meanwhile, the 0.2 M Na_2SO_4 aqueous solution was filled in the cell as the electrolyte. The light source and density were identical with that in the CO_2 photoreduction experiments.

Photocatalytic CO_2 reduction experiments.

The photocatalytic performance of two compounds was evaluated by applying it to the photocatalytic reduction of CO_2 (CEL-PAEM-D8, AULTT, China). The experiments were carried out in a 100 mL Pyrex flask. A 300 W xenon arc lamp (CEL-PF300-T8, AULTT, China) (photocurrent: 15A) was employed as a visible-light source through a UV-cutoff filter with a wavelength greater than 420 nm, which was installed 10 cm away from the reaction solution. In the system of CO_2 photocatalytic reduction, we put photocatalyst into a mixed solvent of triethanolamine (TEOA, as a sacrificial base) and acetonitrile (1:4 v/v, 50 mL), and used $[Ru(bpy)_3]Cl_2•6H_2O$ (11.3 mg) as

photosensitizer. The products were analyzed by performing gas chromatography (GC7920-TF2Z, AULTT, China). The amount of CO and CH_4 was detected by FID, and the H_2 was analyzed by TCD.

$$\text{CO selectivity} = \frac{n(CO)}{n(CO) + n(H_2) + n(CH_4)} \times 100\%$$

$$\text{TON}_{CO} = \frac{n(CO)}{n(catalyst)} \times 100\%$$

The isotope-labeled experiment was performed using $13CO_2$ instead of $12CO_2$, and the result was analyzed by GC-MS (7890B and 5977B, Agilent).

Quantum yield measurement.

The apparent quantum yield (AQY) for products was measured using the same photochemical experimental setup at different wavelengths of 550, 600 and 650 nm. The incident light density was measured using an ultraviolet radiation meter (FZ-A). The calculation of the apparent quantum yield was according to the following equations:

AQY = Ne/Np×100 %.

Ne= 2×number of evolved (CO + H_2 + CH_4) molecules;

Np= the number of incident photons.

Table S1. The AQYs at different excitation wavelengths for compound 2.

Wavelengths (nm)	Incident light density ($mWcm^{-2}$)	AQE (%)
550	17.25	0.86
600	17.54	0.85
650	17.35	0.68

Recycling experiments.

Reusability and stability are important indicators to evaluate catalyst, after each reaction, the catalyst was recovered by centrifugation and washed several times with deionized water and then dried at 80 ℃ for 12h before the next reaction.

Photograph of the CO_2 reduction devices

Fig. S15. The photograph of the CO_2 photoreduction devices.

Reaction

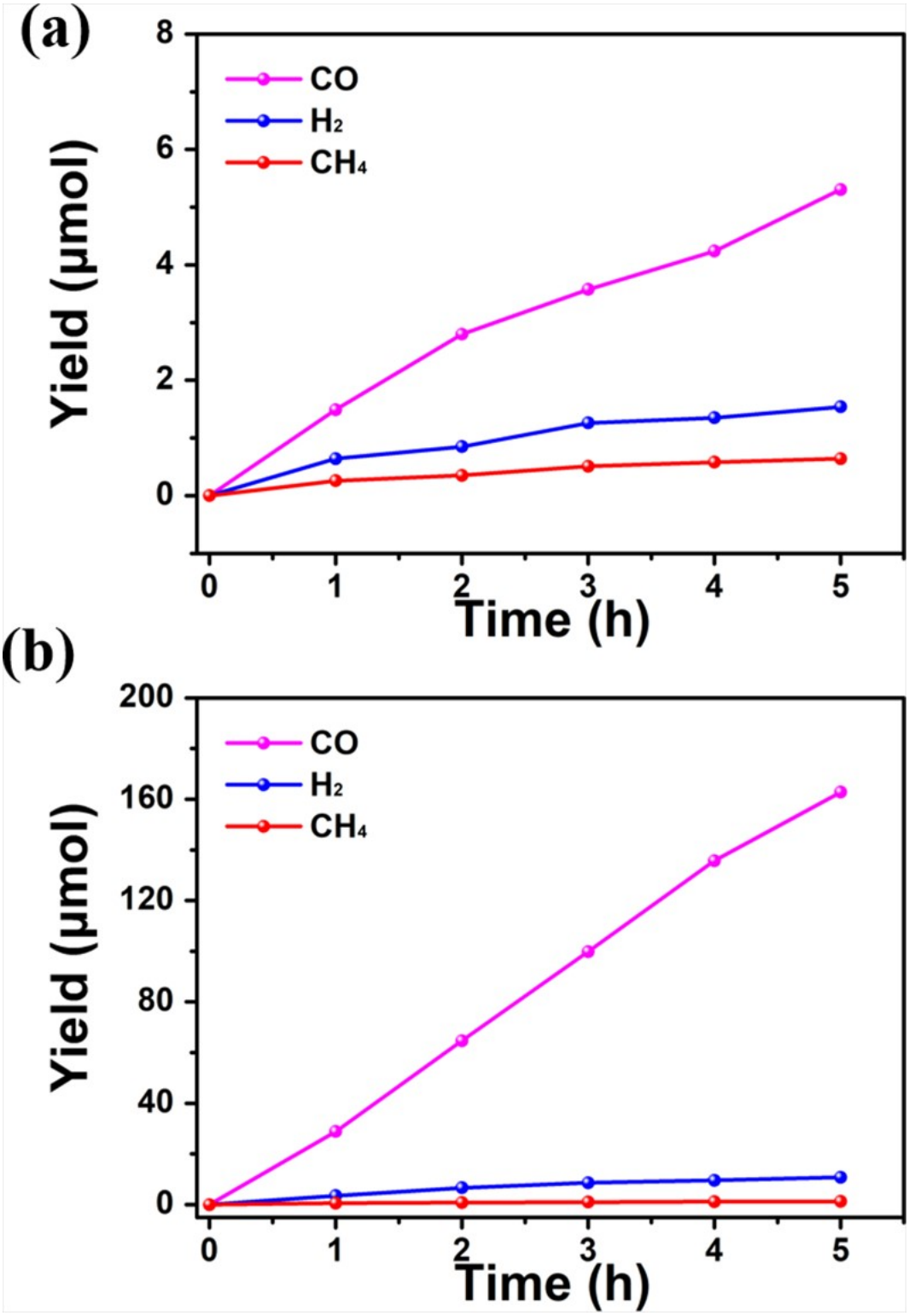

Fig. S16. Time-dependent products generation process of (a) compound **1** and (b) compound **2**.

GC profile

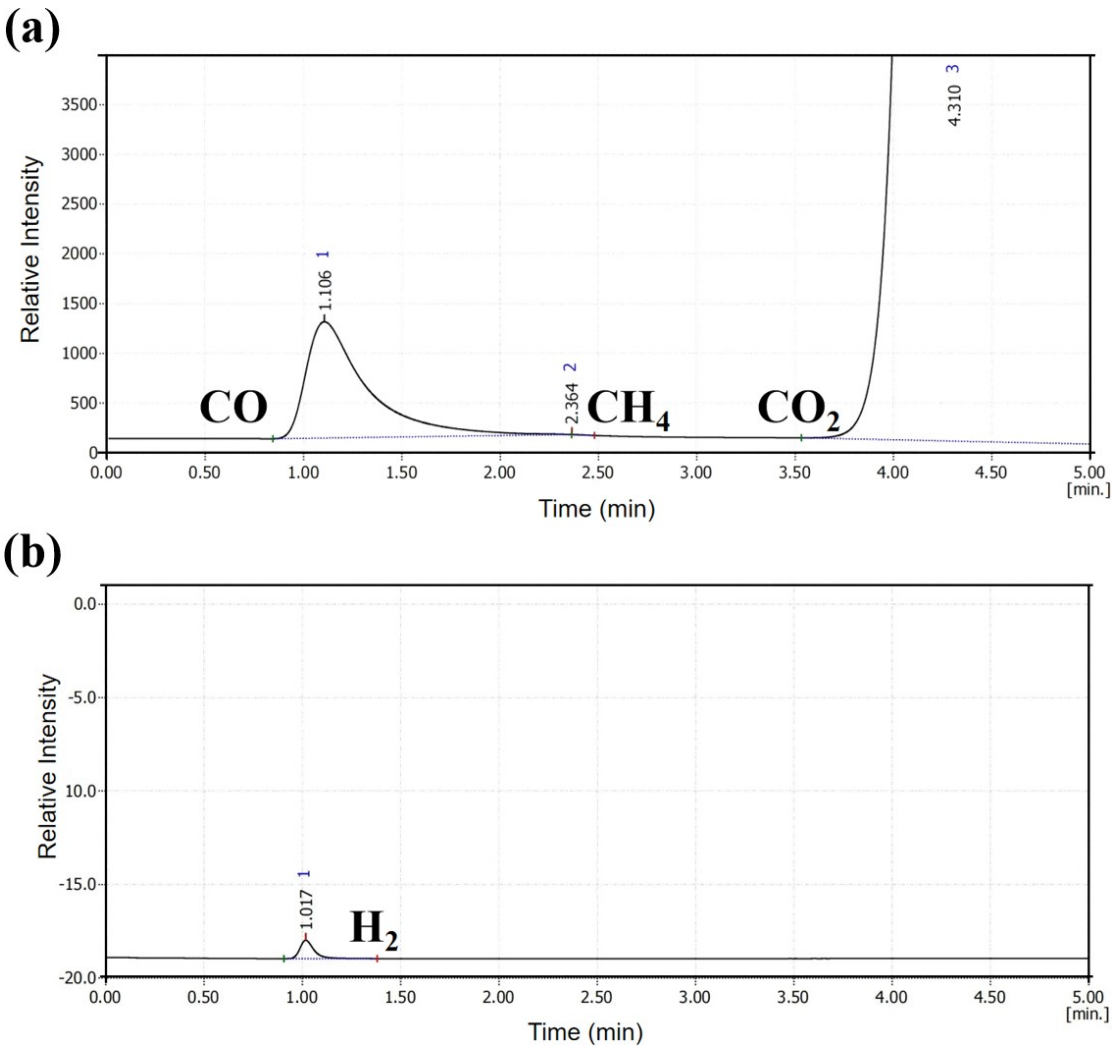

Fig. S17. GC profiles of CO_2 reduction to CO with compound **2** as catalyst after reaction 5 h.

Electrocatalytic CO_2 reduction.

Based on the outstanding performance of compound **2** in CO_2 photoreduction in our manuscript. We carried out detailed research and discussion on the electrochemical measurements, and added the LSV curves of compound **2** electrocatalysts and the Faradaic efficiency (FE) values of compound **2** electrocatalysts at different applied potentials to strengthen our understanding of the CO_2 reduction mechanism.

The activity of compound **2** as electrocatalysts for the electrocatalytic CO_2 reduction reaction (CO_2RR) was examined in a standard three-electrode configuration in 0.5 M $KHCO_3$. Fig. S17 exhibits the linear sweep voltammetry (LSV) curves of the compound **2** in Ar and CO_2 saturated 0.5 M $KHCO_3$ electrolyte, respectively. There is little difference between its current densities in Ar- and CO_2-saturated electrolytes, indicating the no occurrence of the CO_2RR. Fig. S18 shows the FE_{CO} and FE_{H2} of compound **2** at different potentials during the reaction of CO_2 reduction. It is noted that the FE of H_2 on compound **2** reaches above 90% (Fig S19), which is much higher than the FE_{CO} over all the applied potentials, indicating that the electrocatalytic CO_2 reduction reaction is not easy to occur on compound **2**, agreeing well with the results of LSV. As shown is Fig. S20, compound **2** presents the CO reduction currents of -0.01727 mA, -0.02354 mA, -0.06074 mA, -0.21851 mA, -0.48758 mA and -1.05912 mA from -0.6 V to -1.1 V at intervals of 0.1 V, respectively. Meanwhile, the H_2 reduction currents of compound **2** are -0.58085 mA, -0.94148 mA, -2.11831 mA, -3.90493 mA, -6.02948 mA and -8.56647 mA from -0.6 V to -1.1 V at intervals of 0.1 V, respectively. Besides, the overpotential of electrocatalytic CO_2 reduction to CO for compound **2** is 530 mV according to the LSV curves. Although compound **2** has good photocatalytic activity, it has no electrocatalytic activity for CO_2 reduction.

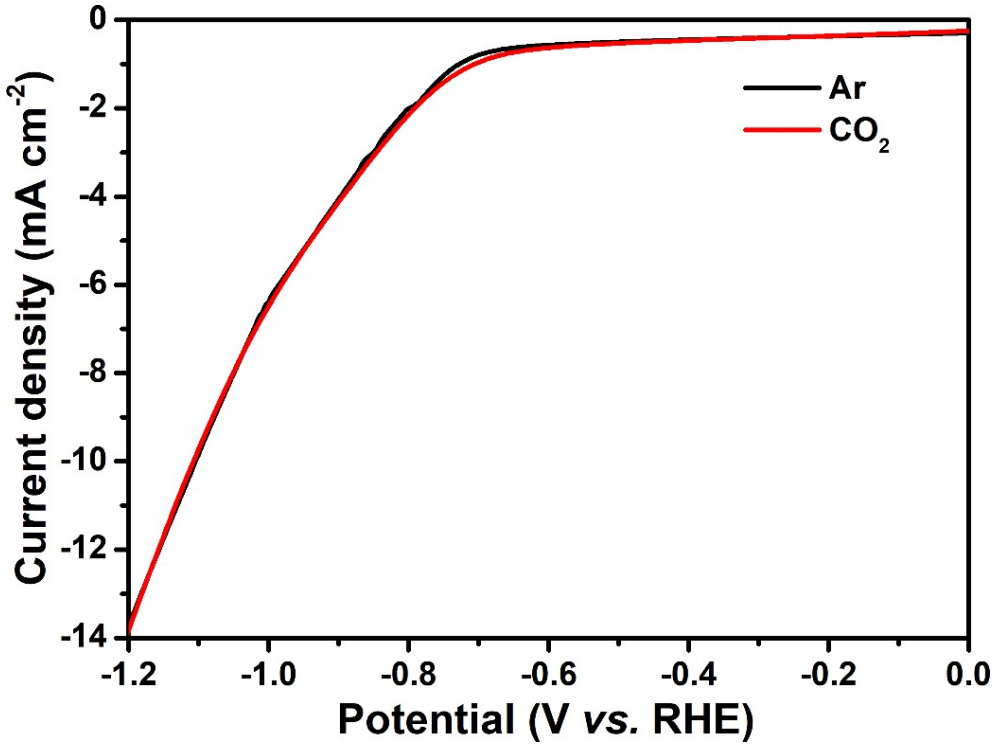

Fig. S18 LSV curves of electrocatalysts in CO_2-saturated 0.5 M $KHCO_3$ electrolyte.

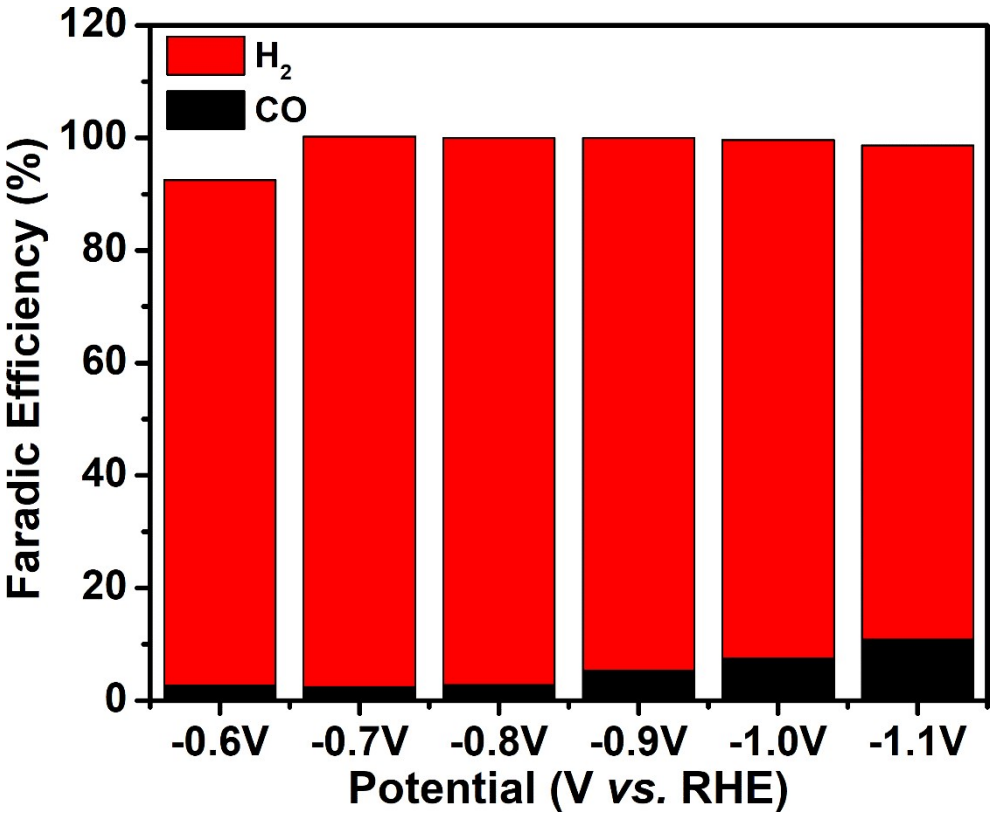

Fig. S19 The FE_{CO} and FE_{H2} values of compound **2** electrocatalysts at different applied potentials in CO_2 saturated 0.5 M $KHCO_3$ electrolyte

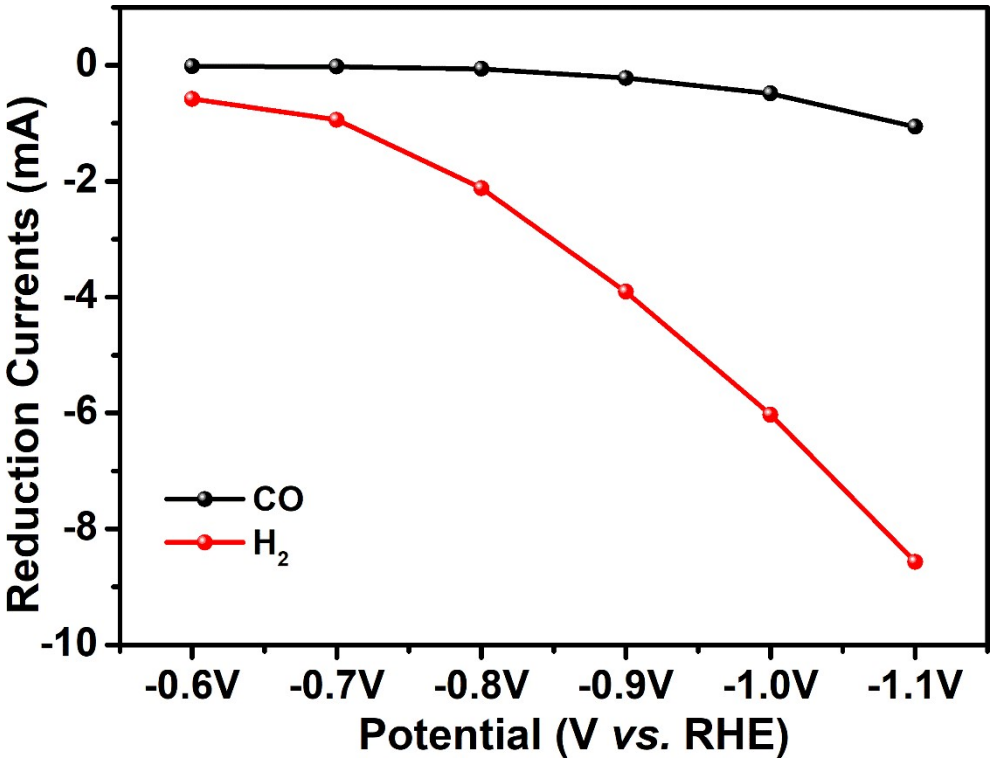

Fig. S20 Partial reduction currents for CO and H_2

Electrocatalytic CO_2 reduction experiments.

All electrocatalysis tests of the catalysts were performed at ambient environment on the electrochemical workstation (SP-150, Bio-Logic) in a standard three-electrode configuration in 0.5 M $KHCO_3$ (pH = 7.2). Pt wire and Ag/AgCl electrodes were used as the counter and reference electrodes, respectively. The experiment was performed in an airtight electrochemical H-type cell with a catalyst-modified carbon cloth electrode (denoted as CCE, 1cm×1cm) as the work electrode.

During the electrocatalytic CO_2 reduction experiments, the polarization curves were performed by linear sweep voltammetry (LSV) mode at a scan rate of 5 mV s^{-1}. Initially, polarization curves for the modified electrode were recorded under Ar atmosphere. Then, the solution was bubbled with CO_2 for at least 30 min to make aqueous solution saturated and the CO_2RR was conducted. All the potential was measured versus Ag/AgCl electrode, and the results were reported versus reversible hydrogen electrode based on the Nernst equation:

E (vs. RHE) = E (vs. Ag/AgCl) + 0.1989 V + 0.0596 × pH

The electrocatalytic CO_2 reduction experiments were carried out under the potential window range from -0.6 V to -1.1 V (vs. RHE) to obtain the reduction products. The gas product obtained is analyzed by online gas chromatography (7820A, Agilent). The faradaic efficiencies (FEs) were calculated using the following equation:

$$FE = \frac{I}{I_t} = \frac{nfxv}{I_t} \times 100$$

Where I = Partial current density of a specific product, A; I_t = total current used in bulk electrolysis, A; n = The number of electrons involved for reduction products; F = Faraday's constant, 96485 C/mol; x = mole fraction of product; V = total molar flow rate of gas.

The overpotential were calculated using the following equation:

Overpotential(mv)=the relative equilibrium potential of (CO_2/CO)-onset potential

Section 4. Other Tables

Table S2. Selected bond lengths (Å) and angles (°) for compound 1.

W(1)-O(4)	1.690(11)	B(2)-O(2)	1.54(2)
W(1)-O(7)#1	1.830(14)	B(2)-O(2)#3	1.54(2)
W(1)-O(3)	1.876(15)	B(2)-O(2)#10	1.54(2)
W(1)-O(5)	1.908(13)	B(2)-O(2)#2	1.54(2)
W(1)-O(3)#2	1.937(14)	B(2)-O(2)#1	1.54(2)
W(1)-O(2)	2.360(17)	Zn(1)-O(17)#11	1.63(2)
W(1)-O(1)	2.441(17)	Zn(1)-O(17)#12	1.63(2)
W(2)-O(8)	1.674(12)	Zn(1)-O(17)#3	1.63(2)
W(2)-O(6)	1.860(14)	Zn(1)-N(1)#6	1.998(16)
W(2)-O(5)	1.868(13)	Zn(1)-N(1)#8	1.998(16)
W(2)-O(6)#1	1.904(15)	Zn(1)-N(1)	1.998(16)
W(2)-O(7)	1.930(12)	Zn(2)-N(4)	1.922(19)
W(2)-O(2)#3	2.43(2)	Zn(2)-N(7)	1.972(18)
W(2)-O(2)	2.45(2)	Zn(2)-N(6)#13	1.998(19)
W(3)-O(14)	1.694(12)	Zn(2)-O(18)	2.008(15)
W(3)-O(13)	1.892(13)	P(1)-O(18)#14	1.472(18)
W(3)-O(15)#4	1.900(16)	P(1)-O(18)#15	1.472(18)
W(3)-O(15)	1.911(16)	P(1)-O(18)	1.473(18)
W(3)-O(16)	1.913(14)	P(1)-O(17)#14	1.81(3)
W(3)-O(10)#5	2.45(2)	P(1)-O(17)#15	1.81(3)
W(3)-O(10)	2.48(2)	P(1)-O(17)	1.81(3)
W(4)-O(12)	1.684(12)	O(4)-W(1)-O(7)#1	100.0(8)
W(4)-O(16)#4	1.849(16)	O(4)-W(1)-O(3)	98.3(7)
W(4)-O(13)	1.885(15)	O(7)#1-W(1)-O(3)	93.1(7)
W(4)-O(11)	1.901(16)	O(4)-W(1)-O(5)	99.8(7)
W(4)-O(11)#6	1.923(16)	O(7)#1-W(1)-O(5)	88.7(6)
W(4)-O(9)#7	2.43(2)	O(3)-W(1)-O(5)	161.2(8)
W(4)-O(10)	2.43(2)	O(4)-W(1)-O(3)#2	98.0(7)
B(1)-O(10)#8	1.46(2)	O(7)#1-W(1)-O(3)#2	161.8(8)
B(1)-O(10)#7	1.46(2)	O(3)-W(1)-O(3)#2	87.2(9)
B(1)-O(10)#6	1.46(2)	O(5)-W(1)-O(3)#2	85.3(6)
B(1)-O(10)#4	1.46(2)	O(4)-W(1)-O(2)	159.0(7)
B(1)-O(10)#5	1.46(2)	O(7)#1-W(1)-O(2)	66.1(7)
B(1)-O(10)	1.46(2)	O(3)-W(1)-O(2)	98.1(7)
B(1)-O(9)	1.50(4)	O(5)-W(1)-O(2)	65.6(7)
B(1)-O(9)#7	1.50(4)	O(3)#2-W(1)-O(2)	95.8(7)
B(2)-O(1)	1.48(3)	O(4)-W(1)-O(1)	159.4(8)

B(2)-O(1)#9	1.48(3)	O(7)#1-W(1)-O(1)	96.1(8)
B(2)-O(2)#9	1.54(2)	O(3)-W(1)-O(1)	67.9(6)
O(5)-W(1)-O(1)	93.3(7)	O(10)#5-B(1)-O(10)	71.2(8)
O(3)#2-W(1)-O(1)	67.1(6)	O(10)#8-B(1)-O(9)	110.1(8)
O(2)-W(1)-O(1)	41.5(7)	O(10)#7-B(1)-O(9)	69.9(8)
O(8)-W(2)-O(6)	100.7(8)	O(10)#6-B(1)-O(9)	110.1(8)
O(8)-W(2)-O(5)	101.7(7)	O(10)#4-B(1)-O(9)	69.9(8)
O(6)-W(2)-O(5)	91.2(7)	O(2)#9-B(2)-O(2)#1	107.5(7)
O(8)-W(2)-O(6)#1	101.2(7)	O(2)-B(2)-O(2)#1	72.5(7)
O(6)-W(2)-O(6)#1	157.8(11)	O(2)#3-B(2)-O(2)#1	107.5(7)
O(5)-W(2)-O(6)#1	88.2(6)	O(2)#10-B(2)-O(2)#1	72.5(7)
O(8)-W(2)-O(7)	99.7(8)	O(2)#2-B(2)-O(2)#1	180.0
O(6)-W(2)-O(7)	87.9(6)	O(17)#11-Zn(1)-O(17)#12	47(2)
O(5)-W(2)-O(7)	158.4(9)	O(17)#11-Zn(1)-O(17)#3	47(2)
O(6)#1-W(2)-O(7)	84.7(7)	O(17)#12-Zn(1)-O(17)#3	47(2)
O(8)-W(2)-O(2)#3	157.1(7)	O(17)#11-Zn(1)-N(1)#6	85.1(15)
O(6)-W(2)-O(2)#3	65.5(7)	O(17)#12-Zn(1)-N(1)#6	109.8(18)
O(5)-W(2)-O(2)#3	96.9(7)	O(17)#3-Zn(1)-N(1)#6	131.0(16)
O(6)#1-W(2)-O(2)#3	92.6(8)	O(17)#11-Zn(1)-N(1)#8	131.0(17)
O(7)-W(2)-O(2)#3	63.2(7)	O(17)#12-Zn(1)-N(1)#8	85.1(15)
O(8)-W(2)-O(2)	158.9(7)	O(17)#3-Zn(1)-N(1)#8	109.8(19)
O(6)-W(2)-O(2)	95.4(8)	N(1)#6-Zn(1)-N(1)#8	109.0(5)
O(5)-W(2)-O(2)	64.1(6)	O(17)#11-Zn(1)-N(1)	109.8(18)
O(6)#1-W(2)-O(2)	64.6(7)	O(17)#12-Zn(1)-N(1)	131.0(17)
O(7)-W(2)-O(2)	94.6(8)	O(17)#3-Zn(1)-N(1)	85.1(15)
O(2)#3-W(2)-O(2)	43.9(8)	N(1)#6-Zn(1)-N(1)	109.0(5)
O(14)-W(3)-O(13)	101.8(8)	N(1)#8-Zn(1)-N(1)	109.0(5)
O(14)-W(3)-O(15)#4	98.4(8)	N(4)-Zn(2)-N(7)	108.8(8)
O(13)-W(3)-O(15)#4	88.4(6)	N(4)-Zn(2)-N(6)#13	105.9(8)
O(14)-W(3)-O(15)	99.0(8)	N(7)-Zn(2)-N(6)#13	107.0(7)
O(13)-W(3)-O(15)	88.9(7)	N(4)-Zn(2)-O(18)	119.0(7)
O(15)#4-W(3)-O(15)	162.6(12)	N(7)-Zn(2)-O(18)	95.3(7)
O(14)-W(3)-O(16)	98.4(8)	N(6)#13-Zn(2)-O(18)	119.3(7)
O(13)-W(3)-O(16)	159.8(9)	O(18)#14-P(1)-O(18)#15	118.6(3)
O(15)#4-W(3)-O(16)	89.1(7)	O(18)#14-P(1)-O(18)	118.6(3)
O(15)-W(3)-O(16)	87.4(6)	O(18)#15-P(1)-O(18)	118.6(3)
O(14)-W(3)-O(10)#5	158.9(8)	O(18)#14-P(1)-O(17)#14	73.5(10)
O(13)-W(3)-O(10)#5	94.7(8)	O(18)#15-P(1)-O(17)#14	113.9(17)
O(15)#4-W(3)-O(10)#5	95.1(8)	O(18)-P(1)-O(17)#14	101.6(18)
O(15)-W(3)-O(10)#5	68.0(7)	O(18)#14-P(1)-O(17)#15	101.6(18)
O(16)-W(3)-O(10)#5	65.6(7)	O(18)#15-P(1)-O(17)#15	73.5(10)
O(14)-W(3)-O(10)	160.7(7)	O(18)-P(1)-O(17)#15	113.9(17)
O(13)-W(3)-O(10)	66.0(7)	O(17)#14-P(1)-O(17)#15	41.7(17)
O(15)#4-W(3)-O(10)	67.4(7)	O(18)#14-P(1)-O(17)	113.9(17)

O(15)-W(3)-O(10)	95.9(8)	O(18)#15-P(1)-O(17)	101.6(18)
O(16)-W(3)-O(10)	94.6(8)	O(18)-P(1)-O(17)	73.5(10)

Table S3. Selected bond lengths (Å) and angles (°) for compound 2.

W(1)-O(4)	1.697(10)	Co(1)-O(17)#11	1.931(10)
W(1)-O(7)#1	1.840(11)	Co(1)-O(17)#3	1.931(10)
W(1)-O(3)	1.865(11)	Co(1)-O(17)#12	1.931(10)
W(1)-O(5)	1.906(10)	Co(1)-N(1)#6	2.002(12)
W(1)-O(3)#2	1.920(11)	Co(1)-N(1)#8	2.002(13)
W(1)-O(2)	2.367(16)	Co(1)-N(1)	2.002(13)
W(1)-O(1)	2.412(15)	Co(2)-O(18)	1.938(12)
W(2)-O(8)	1.663(9)	Co(2)-N(4)	1.969(14)
W(2)-O(5)	1.849(11)	Co(2)-N(6)#13	1.978(17)
W(2)-O(6)	1.852(10)	Co(2)-N(7)	1.981(14)
W(2)-O(7)	1.925(12)	P(1)-O(18)	1.485(14)
W(2)-O(6)#1	1.938(11)	P(1)-O(18)#14	1.485(14)
W(2)-O(2)#3	2.410(15)	P(1)-O(18)#15	1.485(14)
W(2)-O(2)	2.436(15)	P(1)-O(17)	1.502(10)
W(3)-O(14)	1.683(10)	P(1)-O(17)#14	1.502(10)
W(3)-O(15)	1.879(11)	P(1)-O(17)#15	1.502(10)
W(3)-O(13)	1.886(12)	O(4)-W(1)-O(7)#1	99.2(6)
W(3)-O(16)	1.886(12)	O(4)-W(1)-O(3)	99.6(6)
W(3)-O(15)#4	1.905(11)	O(7)#1-W(1)-O(3)	92.9(5)
W(3)-O(10)#5	2.412(18)	O(4)-W(1)-O(5)	99.4(6)
W(3)-O(10)	2.436(18)	O(7)#1-W(1)-O(5)	88.7(5)
W(4)-O(12)	1.678(10)	O(3)-W(1)-O(5)	160.5(6)
W(4)-O(16)#4	1.869(12)	O(4)-W(1)-O(3)#2	98.4(6)
W(4)-O(13)	1.884(12)	O(7)#1-W(1)-O(3)#2	162.0(6)
W(4)-O(11)	1.885(12)	O(3)-W(1)-O(3)#2	88.2(7)
W(4)-O(11)#6	1.886(11)	O(5)-W(1)-O(3)#2	84.4(5)
W(4)-O(10)	2.388(19)	O(4)-W(1)-O(2)	158.4(5)
W(4)-O(9)#7	2.41(2)	O(7)#1-W(1)-O(2)	66.7(6)
B(1)-O(9)	1.51(4)	O(3)-W(1)-O(2)	97.4(6)
B(1)-O(9)#7	1.51(4)	O(5)-W(1)-O(2)	65.4(6)
B(1)-O(10)#5	1.512(18)	O(3)#2-W(1)-O(2)	95.3(6)
B(1)-O(10)#4	1.512(18)	O(4)-W(1)-O(1)	159.1(7)
B(1)-O(10)#8	1.512(18)	O(7)#1-W(1)-O(1)	97.6(7)
B(1)-O(10)#6	1.512(18)	O(3)-W(1)-O(1)	67.0(5)
B(1)-O(10)#7	1.512(18)	O(5)-W(1)-O(1)	93.5(6)
B(1)-O(10)	1.512(18)	O(3)#2-W(1)-O(1)	66.3(5)
B(2)-O(1)#9	1.50(3)	O(2)-W(1)-O(1)	42.4(6)
B(2)-O(1)	1.50(3)	O(8)-W(2)-O(5)	101.0(6)
B(2)-O(2)#9	1.532(15)	O(8)-W(2)-O(6)	99.0(6)
B(2)-O(2)#3	1.532(15)	O(5)-W(2)-O(6)	91.2(5)
B(2)-O(2)	1.532(15)	O(8)-W(2)-O(7)	99.3(6)

B(2)-O(2)#10	1.533(15)	O(5)-W(2)-O(7)	159.5(7)
B(2)-O(2)#2	1.533(15)	O(6)-W(2)-O(7)	88.5(5)
O(8)-W(2)-O(6)#1	99.4(5)	O(10)#5-B(1)-O(10)	71.1(7)
O(5)-W(2)-O(6)#1	88.7(5)	O(10)#4-B(1)-O(10)	71.1(7)
O(6)-W(2)-O(6)#1	161.3(8)	O(10)#8-B(1)-O(10)	108.9(7)
O(7)-W(2)-O(6)#1	85.0(5)	O(10)#6-B(1)-O(10)	108.9(7)
O(8)-W(2)-O(2)#3	158.1(5)	O(10)#7-B(1)-O(10)	180.0
O(5)-W(2)-O(2)#3	96.4(6)	O(1)#9-B(2)-O(1)	180.0
O(6)-W(2)-O(2)#3	67.4(5)	O(1)#9-B(2)-O(2)#9	69.4(6)
O(7)-W(2)-O(2)#3	64.6(5)	O(1)-B(2)-O(2)#9	110.6(6)
O(6)#1-W(2)-O(2)#3	94.0(6)	O(1)#9-B(2)-O(2)#3	69.4(6)
O(8)-W(2)-O(2)	158.3(5)	O(1)-B(2)-O(2)#3	110.6(6)
O(5)-W(2)-O(2)	64.6(5)	O(2)#9-B(2)-O(2)#3	108.4(6)
O(6)-W(2)-O(2)	97.5(6)	O(1)#9-B(2)-O(2)	110.6(6)
O(7)-W(2)-O(2)	95.1(6)	O(1)-B(2)-O(2)	69.4(6)
O(6)#1-W(2)-O(2)	65.7(5)	O(17)#11-Co(1)-O(17)#3	36.3(8)
O(2)#3-W(2)-O(2)	43.5(6)	O(17)#11-Co(1)-O(17)#12	36.3(8)
O(14)-W(3)-O(15)	99.1(6)	O(17)#3-Co(1)-O(17)#12	36.3(8)
O(14)-W(3)-O(13)	99.9(6)	O(17)#11-Co(1)-N(1)#6	101.6(9)
O(15)-W(3)-O(13)	87.9(5)	O(17)#3-Co(1)-N(1)#6	129.0(7)
O(14)-W(3)-O(16)	99.6(6)	O(17)#12-Co(1)-N(1)#6	93.6(8)
O(15)-W(3)-O(16)	88.6(5)	O(17)#11-Co(1)-N(1)#8	93.6(8)
O(13)-W(3)-O(16)	160.5(7)	O(17)#3-Co(1)-N(1)#8	101.6(9)
O(14)-W(3)-O(15)#4	99.6(6)	O(17)#12-Co(1)-N(1)#8	129.0(7)
O(15)-W(3)-O(15)#4	161.3(8)	N(1)#6-Co(1)-N(1)#8	110.3(4)
O(13)-W(3)-O(15)#4	89.4(5)	O(17)#11-Co(1)-N(1)	129.0(7)
O(16)-W(3)-O(15)#4	87.7(5)	O(17)#3-Co(1)-N(1)	93.6(8)
O(14)-W(3)-O(10)#5	158.7(6)	O(17)#12-Co(1)-N(1)	101.6(9)
O(15)-W(3)-O(10)#5	66.9(6)	N(1)#6-Co(1)-N(1)	110.3(4)
O(13)-W(3)-O(10)#5	95.8(6)	N(1)#8-Co(1)-N(1)	110.3(4)
O(16)-W(3)-O(10)#5	65.3(6)	O(18)-Co(2)-N(4)	122.3(6)
O(15)#4-W(3)-O(10)#5	94.9(6)	O(18)-Co(2)-N(6)#13	116.7(6)
O(14)-W(3)-O(10)	158.8(6)	N(4)-Co(2)-N(6)#13	105.1(6)
O(15)-W(3)-O(10)	96.1(6)	O(18)-Co(2)-N(7)	96.1(6)
O(13)-W(3)-O(10)	65.9(6)	N(4)-Co(2)-N(7)	107.9(5)
O(16)-W(3)-O(10)	95.5(7)	N(6)#13-Co(2)-N(7)	107.2(6)
O(15)#4-W(3)-O(10)	66.1(6)	O(18)-P(1)-O(18)#14	114.0(5)
O(10)#5-W(3)-O(10)	42.5(7)	O(18)-P(1)-O(18)#15	114.0(5)
O(12)-W(4)-O(16)#4	98.4(6)	O(18)#14-P(1)-O(18)#15	114.0(5)
O(12)-W(4)-O(13)	99.5(6)	O(18)-P(1)-O(17)	83.0(7)
O(16)#4-W(4)-O(13)	89.2(5)	O(18)#14-P(1)-O(17)	129.9(10)
O(12)-W(4)-O(11)	99.3(6)	O(18)#15-P(1)-O(17)	98.4(14)
O(16)#4-W(4)-O(11)	89.0(5)	O(18)-P(1)-O(17)#14	98.4(14)
O(13)-W(4)-O(11)	161.2(6)	O(18)#14-P(1)-O(17)#14	83.0(7)

O(12)-W(4)-O(11)#6	100.5(6)	O(18)#15-P(1)-O(17)#14	129.9(10)
O(16)#4-W(4)-O(11)#6	161.1(6)	O(17)-P(1)-O(17)#14	47.2(10)

Table S4. The comparison of production of CO for the reported POM-based materials in CO_2 photoreduction system.

Catalyst	Main product	Side product	Efficiency of main product (μmol g^{-1} h^{-1})	Ref
$[Co_4(PO_4)(C_7H_8N_4)_6][BW_{12}O_{40}]\cdot 1.5H_2O$	CO	H_2	10852	**This work**
$H_{26.5}K_{2.5}Na(H_2O)_{16}[Ni_6(OH)(BO_3)_2(dien)_2(B\text{-}\alpha\text{-}SiW_{10}O_{37})_2]_2\cdot 24H_2O$	CO	H_2	6988	1
$[Co(en)_2]_6[V_{12}B_{18}O_{54}(OH)_6]\cdot 17H_2O$	CO	H_2	5700	2
$(H_2bbi)_2\{[Co_2(bbi)][Co_{2.33}(H_2O)_4][H_{9.33}CoP_8Mo_{12}O_{62}]\}\cdot 4H_2O$	CO	CH_4	3261	3
$Na_6[Co(H_2O)_2(H_2tib)]_2\{Co[Mo_6O_{15}(HPO_4)_4]_2\}\cdot 5H_2O$	CO	CH_4	1.09	4

Table S5. The comparison of production of CO for the reported MOF-based materials in CO_2 photoreduction system.

Catalyst	**Main product**	**Side product**	**Efficiency of main product ($\mu mol\ h^{-1}$)**	**Ref**
$Ni_3(HITP)_2$	CO	H_2	34500	5
$[Co_4(PO_4)(C_7H_8N_4)_6][BW_{12}O_{40}]\cdot 1.5H_2O$	CO	H_2	10852	**This work**
2D-M_2TCPE	CO	H_2	4174	6
ZIF-67-3	CO	H_2	3890	7
ZIF-67-1	CO	H_2	3750	
ZIF-67-2	CO	H_2	3060	
Co-UiO-67	CO	H_2	3292.5	8
Re-UiO-67	CO	H_2	412.5	
$\{Co_3(TCA)_2(dpe)_3(H_2O)_6\}$n	CO	H_2	1265.0	9
$\{Ni_3(TCA)_2(dpe)_3(H_2O)_6\}_n$	CO	H_2	371.6	
$\{Cu_3(TCA)_2(dpe)_3(H_2O)_3\}_n$	H_2	CO	232.0	
1-DMF	CO	none	56	10

Reference

(1) Y. Chen, Z. W. Guo, Y. P. Chen, Z. Y. Zhuang, G. Q. Wang, X. X. Li, S. T. Zheng, G. Y. Yang, *Inorg. Chem. Front.*, 2021, **8**, 1303-1311.

(2) X. Yu, C. C. Zhao, J. X. Gu, C. Y. Sun, H. Y. Zheng, L. K. Yan, M. Sun, X. L. Wang, Z. M. Su, *Inorg. Chem.*, 2021, **60**, 7364-7371.

(3) J. N. Li, Z. Y. Du, N. F. Li, Y. M. Han, T. T. Zang, M. X. Yang, X. M. Liu, J. L. Wang, H. Mei, Y. Xu, *Dalton. Trans.*, 2021, **50**, 9137-9143.

(4) J. Du, Y. Y. Ma, X. Xin, H. Na, Y. N. Zhao, H. Q. Tan, Z. G. Han, Y. G. Li, Z. H. Kang, *Chem. Eng. J.*, 2020, **398**, 125518.

(5) W. Zhu, C. F. Zhang, Q. Li, L. K. Xiong, R. X. Chen, X. B. Wan, Z. Wang, W. Chen, Z. Deng, Y. Peng, *Appl. Catal. B: Environ.,* 2018, **238**, 339-345.

(6) H. L. Zheng, S. L. Huang, M. B. Luo, Q. Wei, E. X. Chen, L. He, Q. P. Lin, *Angew. Chem., Int. Ed.*, 2020, **59**, 23588-23592.

(7) M. Wang, J. X. Liu, C. M. Guo, X. S. Gao, C. H. Gong, Y. Wang, B. Liu, X. X. Li, G. G. Gurzadyan, L. C. Sun, *J. Mater. Chem. A.*, 2018, **6**, 4768-4775.

(8) X. S. Gao, B. Guo, C. M. Guo, Q. S. Meng, J. Liang, J. X. Liu, *ACS Appl. Mater. Interfaces*, 2020, 12, 24059-24065.

(9) X. K. Wang, J. Liu, L. Zhang, L. Z. Dong, S. L. Li, Y. H. Kan, D. S. Li, Y. Q. Lan, *ACS Catal*., 2019, **9**, 1726-1732.

(10) Q. Li, Y. P. Luo, Y. Ding, Y. N. Wang, Y. X. Wang, H. B. Du, R. X. Yuan, J. C. Bao, M. Fang, Y. Wu, *Dalton Trans.*, 2019, **48**, 8678-8692.